Synthesis and Properties of Soluble Trifluoromethyl-Substituted Polyimides Containing Laterally Attached *p*-Terphenyls

SHENG-HUEI HSIAO, YU-HUI CHANG

Department of Chemical Engineering, Tatung University, 40 Chungshan North Road, Section 3, Taipei 104, Taiwan, Republic of China

Received 20 August 2003; accepted 13 November 2003

ABSTRACT: A new fluorinated diamine monomer, 2′,5′-bis(4-amino-2-trifluoromethylphenoxy)-*p*-terphenyl, was synthesized from the chloro-displacement of 2-chloro-5-nitrobenzotrifluoride with the potassium phenolate of 2,5-diphenylhydroquinone, followed by hydrazine palladium-catalyzed reduction. A series of trifluoromethyl-substituted polyimides containing flexible ether linkages and laterally attached side rods were synthesized from the diamine with various aromatic dianhydrides via a conventional two-step process. The inherent viscosities of the poly(amic acid) precursors were 0.84–1.26 dL/g. All the polyimides afforded flexible and tough films. The use of 4,4′-oxydiphthalic anhydride and 2,2′-bis(3,4-dicarboxyphenyl)hexafluoropropane dianhydride produced essentially colorless polyimide films. Most of the polyimides revealed an excellent solubility in many organic solvents. The glass-transition temperatures of these polyimides were recorded between 254 and 299 °C by differential scanning calorimetry, and the softening temperatures of the polymer films stayed in the range of 253–300 °C according to thermomechanical analysis. The polyimides did not show significant decomposition before 500 °C in air or under nitrogen. These polyimides also showed low dielectric constants (2.83–3.34 at 1 MHz) and low moisture absorption (0.4–2.2%). For a comparative study, a series of analogous polyimides based on the nonfluorinated diamine 2′,5′-bis(4-aminophenoxy)-*p*-terphenyl were also prepared and characterized. J Polym Sci Part A: Polym Chem 42: 1255–1271, 2004

Keywords: new trifluoromethyl-containing diamine; polyimides; fluoropolymers; high performance polymers; *p*-terphenyl; organosoluble; thermal properties; dielectric properties; structure-property relations

INTRODUCTION

Aromatic polyimides are well known as high-performance polymeric materials for their outstanding thermal, mechanical, and electrical properties and excellent chemical resistance.[1,2] However, their limited solubility and infusibility restrict their applications in some fields. Therefore, much research has been focused on the preparation of soluble or thermoplastic polyimides without the loss of their desirable properties.[3,4] Typical approaches include the incorporation of flexible linkages,[5–7] bulky lateral or cardo groups,[8–11] kinked or unsymmetrical structures,[12–15] and spiro-skeletons[16–20] into the polymer backbone.

Rigid-rod aromatic polymers containing *p*-terphenyl segments in the main chain are generally insoluble and infusible. Several soluble rigid-rod polyamides and polyimides have been prepared

Correspondence to: S.-H. Hsiao (E-mail: shhsiao@ttu.edu.tw)

Journal of Polymer Science: Part A: Polymer Chemistry, Vol. 42, 1255–1271 (2004)

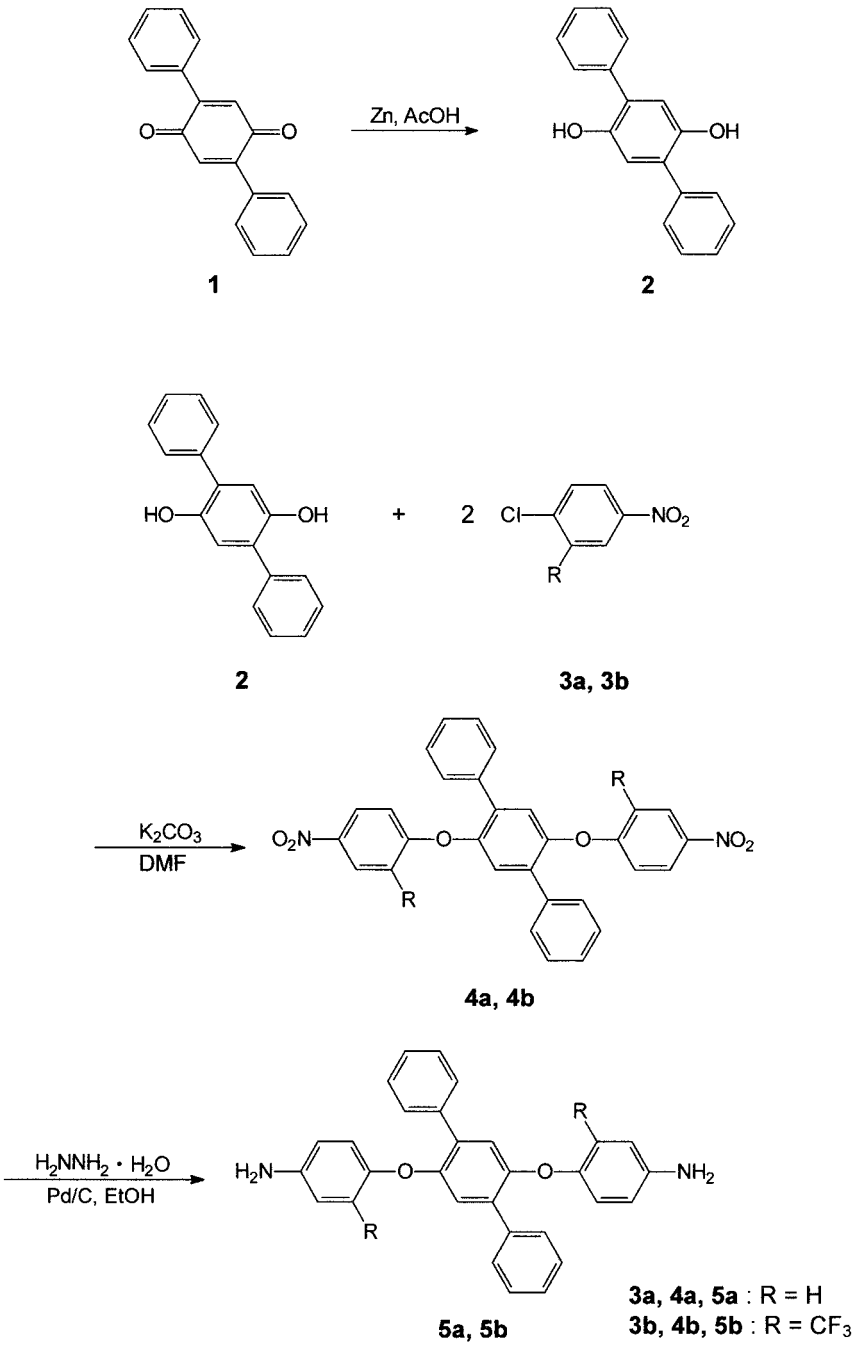

Scheme 1. Synthetic routes for diamines **5a** and **5b**.

from aromatic diamines of *p*-terphenyl bearing bulky pendent substituents.[21–24] There have been reports on thermotropic liquid-crystalline and light-emitting polymers containing *p*-terphenyl or its analogues in the main chain.[25,26] Recently, Xu et al.[27] studied polyimides derived from 2′,5′-bis(4-aminophenoxy)-*p*-terphenyl (**5a**; see Scheme 1) with commercial dianhydrides in an effort to enhance the solubility. The lateral arrangement of *p*-terphenyl in the polyimide backbone was expected to interrupt interchain packing and increase solubility. However, unless 2,2′-bis(3,4-dicarboxyphenyl)hexafluoropropane dianhydride (6FDA) was incorporated, the polyimides from **5a** were not organosoluble. Fluorinated polyimides are well known to display a

number of unique properties, and there are several excellent reference sources available.[28,29] Polyimides containing the trifluoromethyl (CF_3) group attached to the polymer backbone have lower dielectric constants and water absorption along with higher solubility and optical transparency than observed for the nonfluorinated analogues.[30–33] This work is focused on the synthesis of a novel CF_3-substituted diamine, 2′,5′-bis(4-amino-2-trifluoromethylphenoxy)-*p*-terphenyl (**5b**; see Scheme 1), and its derived fluorinated polyimides. The basic properties of the fluorinated polyimides containing laterally attached *p*-terphenyls were investigated and compared to those of analogous counterparts prepared from a structurally similar, nonfluorinated diamine (**5a**). The polyimides of **5b** were expected to exhibit more enhanced solubility and diminished dielectric constants because of the increased free volume caused by the CF_3 groups.[34]

EXPERIMENTAL

Materials

2,5-Diphenyl-*p*-benzoquinone (**1**; Lancaster), 1-chloro-4-nitrobenzene (**3a**; TCI), 2-chloro-5-nitrobenzotrifluoride (**3b**; Lancaster), potassium carbonate (K_2CO_3; Fluka), 10% palladium on charcoal (Pd/C; Fluka), and hydrazine monohydrate (Acros) were used as received. Commercially available aromatic tetracarboxylic dianhydrides such as pyromellitic dianhydride (PMDA or **6a**; Aldrich), 3,3′,4,4′-benzophenonetetracarboxylic dianhydride (BTDA or **6c**; Aldrich), 4,4′-oxydiphthalic dianhydride (ODPA or **6d**; Oxychem), and 3,3′4,4′-diphenylsulfonetetracarboxylic dianhydride (DSDA or **6e**; New Japan Chemical Co.) were purified by recrystallization from acetic anhydride. 3,3′,4,4′-Biphenyltetracarboxylic dianhydride (BPDA or **6b**; Oxychem) and 6FDA (**6f**; Hoechst Celanese) were purified by vacuum sublimation. *N,N*-Dimethylacetamide (DMAc) was purified by distillation under reduced pressure over calcium hydride (CaH_2) and stored over 4-Å molecular sieves.

Monomer Synthesis

*2,5-Diphenylhydroquinone (2,5-Dihydroxy-*p*-terphenyl or 2)*

In a 1-L, round-bottom flask equipped with a stirring bar and a condenser, a mixture of 25 g (0.096 mol) of **1** and 12 g of Zn powder in 500 mL of acetic acid was refluxed for 5 h. The resulting transparent, pale yellow solution was filtered while hot, and 1 L of water was added to the filtrate. The resulting precipitate was filtered, collected, and dried as a light yellow solid [21.6 g, 86%; mp = 223–225 °C according to differential scanning calorimetry (DSC) at a scanning rate of 2 °C/min].

IR (KBr): 3539 (free O—H stretching), 3438 (hydrogen-bonded O—H stretching), 1182, 1143 cm^{-1} (C—O stretching). ^1H NMR [dimethyl sulfoxide-d_6 (DMSO-d_6), δ, ppm]: 8.95 (s, 2H, —OH), 7.57 (dd, J = 8.0, 0.9 Hz, 4H, H_b), 7.41 (dd, J = 7.5, 7.8 Hz, 4H, H_c), 7.29 (t, J = 7.4 Hz, 2H, H_d), 6.88 (s, 2H, Ha). ^{13}C NMR (DMSO-d_6, δ, ppm): 147.0 (C^1), 138.3 (C^4), 128.8 (C^6), 127.9 (C^5), 126.4 (C^3), 125.2 (C^7), 117.4 (C^2).

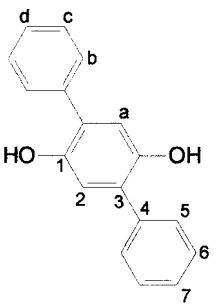

ELEM. ANAL. Calcd. for $C_{18}H_{14}O_2$ (262.31): C, 82.42%; H, 5.38%. Found: C, 82.78%; H, 5.28%.

*2′,5′-Bis(4-nitrophenoxy)-*p*-terphenyl (4a)*

In a 250-mL, round-bottom flask, 11.6 g (0.044 mol) of **2** and 13.9 g (0.088 mol) of **3a** were dissolved in 100 mL of *N,N*-dimethylformamide (DMF). Then, 12.2 g (0.088 mol) of potassium carbonate was added, and the suspension solution was refluxed at 150 °C for 8 h. After cooling, the mixture was poured into 400 mL of methanol/water (1:2 v/v), and the precipitated light yellow solid was collected by filtration and washed thoroughly with methanol and water. The crude product was recrystallized from DMF/methanol to afford 17.2 g (78% yield) of fluffy, yellowish, fine needles (mp = 275–276 °C according to DSC at 2 °C/min, lit.[27] 276–277.5 °C).

IR (KBr): 1513 (N═O asymmetric stretching), 1344 (N═O symmetric stretching), 1236 cm^{-1} (C—O stretching). ELEM. ANAL. Calcd. for $C_{30}H_{20}N_2O_6$ (504.50): C, 71.42%; H, 4.00%; N, 5.55%. Found: C, 71.48%; H, 3.98%; N, 5.57%.

2′,5′-Bis(4-aminophenoxy)-p-*terphenyl (5a)*

A mixture of dinitro compound **4a** (15.67 g, 0.03 mol), 10% Pd/C (0.2 g), hydrazine monohydrate (10 mL), and ethanol (200 mL) was heated at a reflux temperature for 4 h. After the mixture cooled, 100 mL of DMF was added to dissolve the precipitated product, and the reaction solution was filtered to remove Pd/C. The filtrate was added to 300 mL of water, and then the resulting off-white precipitate was collected by filtration and dried *in vacuo* at 120 °C overnight. The yield was 12 g (87%; mp = 250–251 °C according to DSC at 2 °C/min, lit.[27] 251–252 °C).

IR (KBr): 3444, 3361 (N—H stretching), 1211 cm^{-1} (C—O stretching). ^1H NMR (DMSO-d_6, δ, ppm): 7.50 (dd, J = 7.2, 1.4 Hz, 4H, H_b), 7.38 (dd, J = 7.2, 7.6 Hz, 4H, H_c), 7.30 (t, J = 7.6 Hz, 2H, H_d), 6.83 (s, 2H, H_a), 6.77 (d, J = 8.8 Hz, 4H, H_e), 6.56 (d, J = 8.8 Hz, 4H, H_f), 4.88 (s, 4H, —NH_2). ^{13}C NMR (DMSO-d_6, δ, ppm): 150.1 (C^1), 146.8 (C^8), 144.8 (C^{11}), 136.8 (C^4), 131.4 (C^3), 128.7 (C^6), 128.4 (C^5), 127.3 (C^7), 119.7 (C^9), 119.5 (C^2), 114.9 (C^{10}).

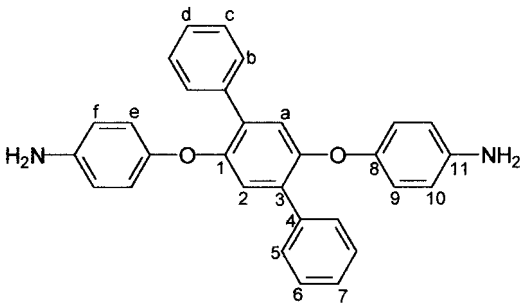

ELEM. ANAL. Calcd. for $C_{30}H_{24}N_2O_2$ (444.53): C, 81.06%; H, 5.44%; N, 6.30%. Found: C, 80.89%; H, 5.50%; N, 6.24%.

2′,5′-Bis(2-trifluoromethyl-4-nitrophenoxy)-p-*terphenyl (4b)*

In a 250-mL, round-bottom flask, 13.1 g (0.05 mol) of **2** and 22.6 g (0.1 mol) of **3b** were dissolved in 100 mL of DMF. Then, 13.8 g (0.1 mol) of potassium carbonate was added, and the suspension solution was heated at 120 °C for 6 h. After cooling, the mixture was poured into 400 mL of methanol/water (1:2 v/v), and the precipitated light yellow solid was collected by filtration and washed thoroughly with methanol and water. The crude product was recrystallized from DMF/methanol to afford 28.5 g (89% yield) of fluffy, light yellow, fine needles (mp = 261–262 °C according to DSC at 2 °C/min).

IR (KBr): 1526 (N═O asymmetric stretching), 1350 (N═O symmetric stretching), 1254 (C—O stretching), 1157 cm^{-1} (C—F stretching). ^1H NMR (DMSO-d_6, δ, ppm): 8.43 (d, J = 2.7 Hz, 2H, H_g), 8.35 (dd, J = 9.3, 2.7 Hz, 2H, H_f), 7.57 (s, 2H, H_a), 7.53 (d, J = 6.8 Hz, 4H, H_b), 7.36 (dd, J = 7.5, 7.5 Hz, 4H, H_c), 7.33 (t, J = 7.0 Hz, 2H, H_d), 7.25 (d, J = 9.3 Hz, 2H, H_e).

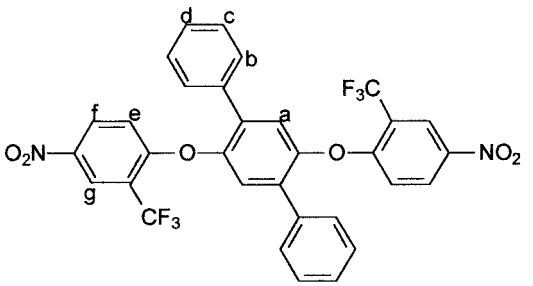

ELEM. ANAL. Calcd. for $C_{32}H_{18}N_2O_6F_6$ (640.49): C, 60.01%; H, 2.83%; N, 4.37%. Found: C, 60.03%; H, 2.75%; N, 4.32%.

2′,5′-Bis(4-amino-2-trifluoromethylphenoxy)-p-*terphenyl (5b)*

A mixture of dinitro compound **4b** (15 g, 0.023 mol), 10% Pd/C (0.2 g), hydrazine monohydrate (10 mL), and ethanol (250 mL) was heated at a reflux temperature for 4 h. The reaction solution was filtered while hot to remove Pd/C. After cooling, the off-white crystals were collected by filtration and dried *in vacuo* at 120 °C overnight. The yield was 11.1 g (81%; mp = 222–223 °C according to DSC at 2 °C/min).

IR (KBr): 3489, 3427, 3394, 3320, 3226 (N—H stretching), 1261 (C—O stretching), 1124 cm^{-1} (C—F stretching). ^1H NMR (DMSO-d_6, δ, ppm): 7.51 (dd, J = 7.9, 1.4 Hz, 4H, H_b), 7.41 (dd, J = 7.9, 7.2 Hz, 4H, H_c), 7.33 (t, J = 7.2 Hz, 2H, H_d), 6.93 (d, J = 2.6 Hz, 2H, H_g), 6.90 (d, J = 8.8 Hz, 2H, H_e), 6.81 (s, 2H, H_a), 6.80 (dd, J = 2.6, 8.8 Hz, 2H, H_f), 5.40, 5.38 (—NH_2). ^{13}C NMR (DMSO-d_6, δ, ppm): 149.7 (C^1), 145.1 (C^8), 143.1 (C^{11}), 136.2 (C^4), 131.7 (C^3), 128.7 (C^6), 128.3 (C^5), 127.6 (C^7), 123.5 (quartet, $^1J_{C—F}$ = 271 Hz, C^{14}), 121.4 (C^9), 120.5 (quartet, $^2J_{C—F}$ = 30 Hz, C^{13}), 119.3 (C^2), 118.7 (C^{10}), 110.8 (C^{12}).

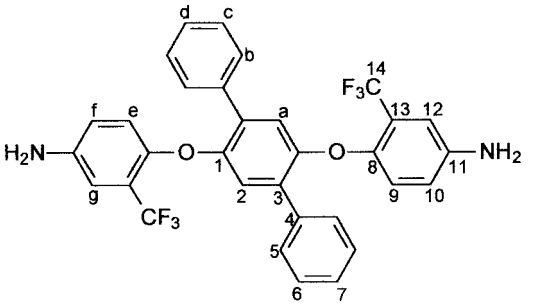

ELEM. ANAL. Calcd. for $C_{32}H_{22}N_2O_2F_6$ (580.53): C, 66.21%; H, 3.82%; N, 4.82%. Found: C, 66.31%; H, 3.66%; N, 4.65%.

Polymer Synthesis

The synthesis of polyimide **10b** is used as an example to illustrate the general synthetic route used to produce the polyimides. To a solution of 1.3272 g (2.28 mmol) of diamine **5b** in 19 mL of CaH_2-dried DMAc in a 50-mL, round-bottom flask, 0.6728 g (2.28 mmol) of dianhydride BPDA was added in one portion. The mixture was stirred at room temperature overnight (for ca. 10 h) to afford a viscous poly(amic acid) solution. The inherent viscosity of the resulting poly(amic acid) (**8b**) was 1.26 dL/g. It was subsequently converted into polyimide by either a thermal or chemical imidization process. For the thermal imidization process, about 10 g of the obtained poly(amic acid) solution was poured into a 9-cm glass culture dish, which was placed in a 90 °C oven for the removal of the casting solvent. The semidried poly(amic acid) film was further dried and converted into the polyimide by sequential heating at 150 °C for 30 min, at 200 °C for 30 min, and at 250 °C for 1 h. After cooling, the flexible polyimide film of **10b** was self-stripped from the glass substrate. Chemical imidization was performed through the addition of 2 mL of pyridine and 5 mL of acetic anhydride to the remaining poly(amic acid) solution and the stirring of the mixture at room temperature overnight. The resulting homogeneous polyimide solution was poured into methanol to give a light yellow, fibrous precipitate, which was collected by filtration, washed thoroughly with methanol, and dried. The inherent viscosity of **10b** was 1.33 dL/g in DMAc at a concentration of 0.5 dL/g at 30 °C.

Characterization

IR spectra were recorded on a Horiba FT-720 Fourier transform infrared (FTIR) spectrometer. Elemental analysis was performed on a Heraeus Vario EL-III elemental analyzer. ^1H and ^{13}C NMR spectra were measured on a JEOL EX 400 spectrometer with DMSO-d_6 as the solvent and tetramethylsilane as the internal reference. The inherent viscosities of the poly(amic acid)s and polyimides were determined with an Ubbelohde viscometer at 30 °C. Gel permeation chromatography (GPC) was carried out on a Waters chromatography unit interfaced with a Waters 2410 refractive-index detector. Two Waters 5-μm Styragel HR-2 and HR-4 columns (7.8-mm inside diameter × 300 mm) connected in series were used with tetrahydrofuran (THF) as the eluent and were calibrated with narrow polystyrene standards. The measurements were carried out at 35 °C at a flow rate of 1.0 mL/min. An Instron universal tester (model 1130) with a load cell of 5 kg was used to study the stress–strain behavior of the polyimide film samples. A gauge length of 2 cm and a crosshead speed of 5 mm/min were used for this study. Measurements were performed at room temperature with film specimens (0.5 cm wide, 6 cm long, and ca. 0.08 mm thick), and at least three replicas were used. Wide-angle X-ray diffraction (WAXD) measurements were performed at room temperature (ca. 25 °C) on a Shimadzu XRD-6000 X-ray diffractometer (operating at 40 kV and 30 mA) with graphite-monochromatized Cu Kα radiation (λ = 1.5418 Å). The scanning rate was 2°/min over a range of 2θ= 10–40°. Ultraviolet–visible (UV–vis) spectra of the polymer films were recorded on a Unicam UV300 UV–vis spectrophotometer. Thermogravimetric analysis (TGA) was conducted with a PerkinElmer Pyris 1 TGA instrument. Experiments were carried out with approximately 6–8-mg samples in flowing nitrogen or air (flow rate = 20 cm^3/min) at a heating rate of 20 °C/min. DSC analyses were performed on a PerkinElmer Pyris 1 DSC instrument at a heating rate of 20 °C/min under nitrogen. Glass-transition temperatures (T_g's) were read at the middle of the transition in the heat capacity and were taken from the second heating scan after quick cooling from 400 °C at a cooling rate of 200 °C/min. Thermomechanical analysis (TMA) was conducted with a PerkinElmer TMA 7 instrument. The TMA experiments were conducted from 40 to 300 °C at a scanning rate of 10 °C/min with a penetration probe 1.0 mm in diameter under an applied constant load of 10 mN. Softening temperatures (T_s's) were taken as the onset temperature of probe displacement on the TMA traces. The dielectric property of the poly-

mer films was tested by the parallel-plate capacitor method with an HP-4194A impedance/gain phase analyzer. Gold electrodes were vacuum-deposited on both surfaces of dried films. Experiments were performed at 25 °C in a dry chamber. The equilibrium moisture absorption was determined by the weighing of the changes in vacuum-dried film specimens before and after immersion in deionized water at 25 °C for 72 h.

RESULTS AND DISCUSSION

Monomer Synthesis

The diamine monomers **5a** and **5b** were synthesized via the three-step synthetic route outlined in Scheme 1. According to a reported method,[35] **2** was obtained in a good yield from the reduction of **1** by means of zinc powder in boiling acetic acid. Then, the dinitro intermediates **4a** and **4b** were synthesized by the aromatic chloro-displacement reaction of **3a** and **3b**, respectively, with the potassium phenoxide prepared *in situ* from diol **2** and potassium carbonate in DMF. Both the para nitro group and ortho CF_3 group activated the chlorine for displacement; therefore, the chloro-displacement reaction of **3b** by the potassium phenolate of **2** could be carried out at a mild temperature. The subsequent reduction of the dinitro compounds **4a** and **4b** with the hydrazine hydrate and Pd/C catalyst in refluxing ethanol readily gave diamines **5a** and **5b**. The yields in each step were very high, and the obtained products in each step were confirmed by elemental analysis and spectroscopic techniques. Recently, **5a** was also synthesized by Xu et al.;[27] the diamine was prepared by a bromo-displacement reaction between 1-bromo-4-nitrobenzene and **2** followed by a Pd/C-catalyzed reduction of the resulting dinitro compound with ammonium formate as the reducing agent. This diamine has been used in the synthesis of organosoluble polyimides and copolyimides through a reaction with 6FDA or equimolar mixtures of 6FDA and other dianhydrides such as BPDA, BTDA, ODPA, and DSDA.[27]

The FTIR spectra of compounds **2**, **4b**, and **5b** are given in Figure 1. In the FTIR spectrum of diol **2**, a sharp free (non-hydrogen-bonded) O—H stretching band appears at 3539 cm^{-1} to the left of the broader intermolecular hydrogen-bonded band at 3438 cm^{-1}. The phenomenon implies that the bulky phenyl group ortho to the hydroxyl group may sterically hinder the formation of intermolecular hydrogen bonding. Bands representative of the nitro functionality for the dinitro compound **4b** appear near 1530 (asymmetric stretch) and 1350 cm^{-1} (symmetric stretch). After reduction, the aromatic primary amine absorptions in the region of 3300–3500 cm^{-1} were identified, and the bands for the nitro group were absent. The strong bands at 1100–1160 cm^{-1}, assigned to the C—F stretch, are also apparent in the FTIR spectra of the CF_3-substituted compounds **4b** and **5b**.

The structures were also confirmed by high-resolution NMR spectra. The ^1H NMR spectra confirm that the nitro groups were completely converted into amino groups by the high field shift of the aromatic protons and the signals at 4.88–5.39 ppm corresponding to the primary aromatic amine protons. Figure 2 compares the expanded aromatic ring portions of the ^1H NMR spectra of diamines **5a** and **5b**. Clearly, the aromatic protons (H_e to H_g) on the CF_3-substituted ring of diamine **5b** resonated at a lower field because of the electron-withdrawing CF_3 group. Figure 3 compares the ^{13}C NMR spectra of diamines **5a** and **5b** in DMSO-d_6. The ^{13}C NMR spectrum of diamine **5b** shows two clear quartets due to heteronuclear ^{13}C–^{19}F coupling. The larger quartet centered at about 123.5 ppm was due to the CF_3 carbon. The one-bond C—F coupling constant in this case was about 271 Hz. The CF_3-attached carbon C^{13} also showed a clear quartet centered at about 120.5 ppm with a smaller coupling constant of about 30 Hz due to two-bond C—F coupling. Besides, the C^8 and C^{12} carbons (ortho to the CF_3 group) also have their resonances split by the fluorine atoms (three-bond coupling). The close splitting has an even smaller coupling constant (ca. 5 Hz) because the interaction operates over more bonds. Thus, all the spectroscopic data obtained were in good agreement with the expected structures of all the dinitro and diamino compounds. The NMR spectra of diamine **5a** are similar to those reported.[27] Slightly different chemical shifts of some peaks with respect to the reported values could be attributed to the use of different NMR solvents.

Polymer Synthesis

The new fluorinated polyimides were prepared by the reaction of diamine **5b** with six commercially available dianhydrides (**6a**–**6f**) to form poly(amic acid)s, followed by thermal or chemical imidization. The structures and codes of the prepared polymers are shown in Scheme 2. Despite the

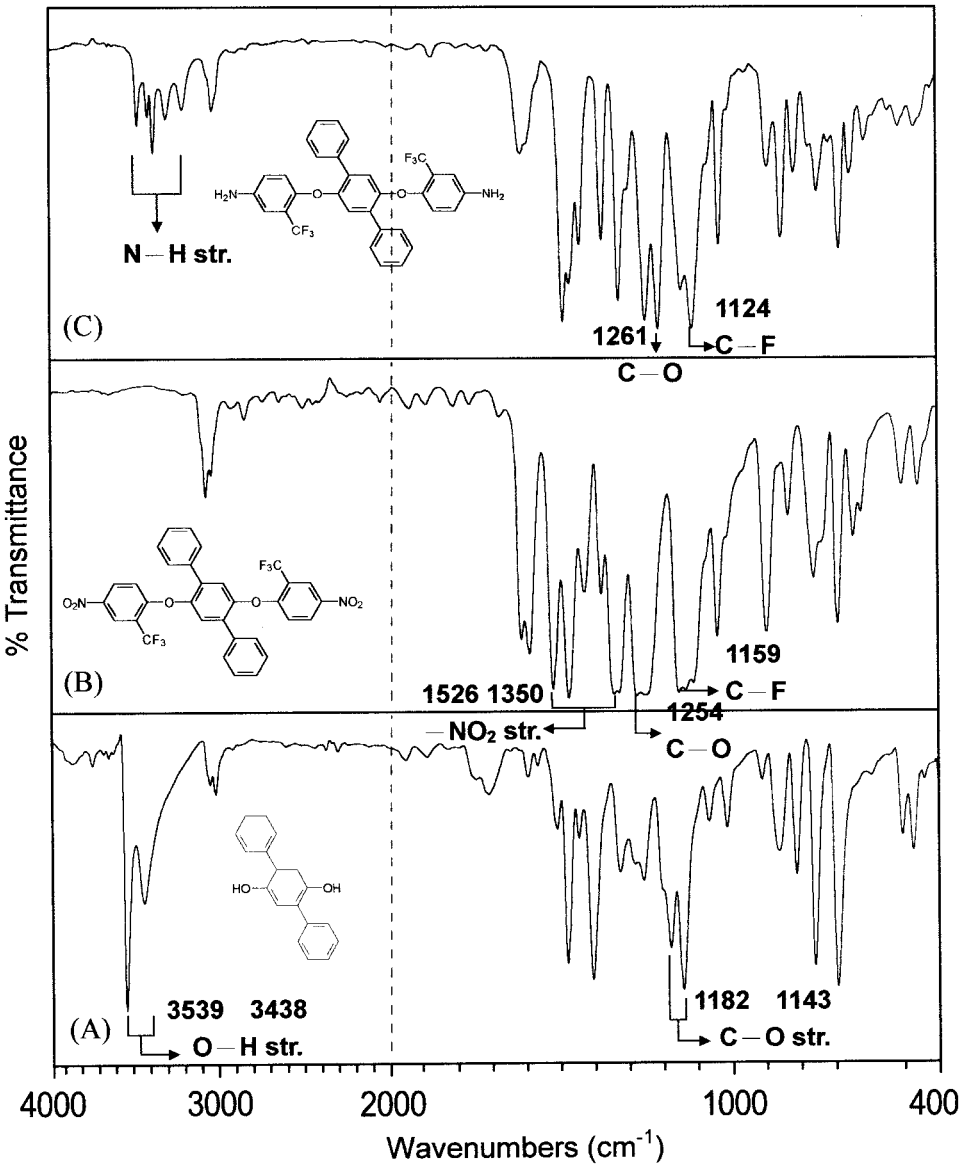

Figure 1. FTIR spectra of (A) diol **2**, (B) dinitro compound **4b**, and (C) diamine **5b**.

presence of electron-withdrawing CF_3 substituents, **5b** was still sufficiently reactive to give high-molecular-weight poly(amic acid)s when allowed to polymerize for a longer time (ca. 12 h). As shown in Table 1, the inherent viscosities of the poly(amic acid)s (**8a–8f**) from **5b** were 0.84–1.26 dL/g. The molecular weights of all these poly(amic acid)s were sufficiently high to permit the casting of flexible and tough poly(amic acid) films, which could be subsequently converted into tough polyimide films by extended heating at elevated temperatures. **5b** mostly likely retained its reactivity because the amino group was meta to the CF_3 group. Except for that derived from rigid PMDA, all the chemically cyclodehydrated fluorinated polyimides exhibited good solubility in polar solvents such as *N*-methyl-2-pyrrolidone (NMP) and DMAc. Therefore, the characterization of the solution viscosity was carried out without any difficulty, and the inherent viscosities of the soluble polyimides (**10b–10f**) were between 0.62 and 1.33 dL/g, as measured in DMAc. As shown in Table 1, the weight-average molecular weights (M_w's) and number-average molecular weights (M_n's) of the THF-soluble polyimides (**10b–10f**) measured by GPC were 67,000–100,000 and 42,000–79,000, respectively, with respect to polystyrene standards. For comparison, a series of reference poly-

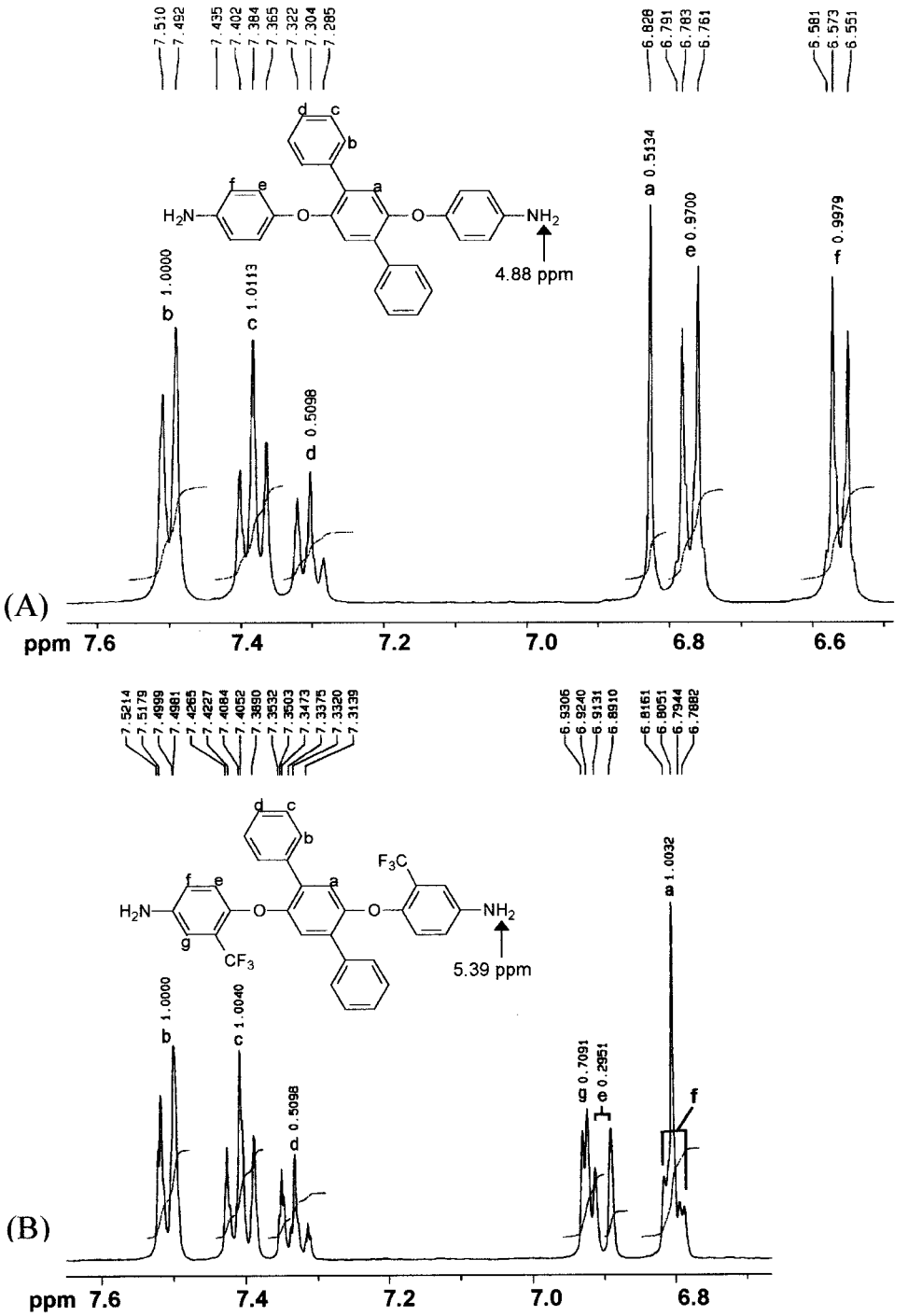

Figure 2. ^{1}H NMR (DMSO-d_6) spectra of (A) diamine **5a** and (B) diamine **5b**.

imides (**9a**–**9f**) were also synthesized from diamine **5a** and dianhydrides **6a**–**6f**. The inherent viscosities of the precursor poly(amic acid)s of **7a** and **7b** were 1.27–3.01 dL/g, indicating the formation of high-molecular-weight polymers. With the exception of polyimide **9a**, all the polyimides (**9b**–**9f**) were obtained as flexible and tough films from the thermal curing of their corresponding poly(amic acid) films. The film of polyimide **9a** was opaque and slightly brittle, probably because of the rigid nature of the polymer backbone caused by the PMDA moieties. Among the **9** series poly-

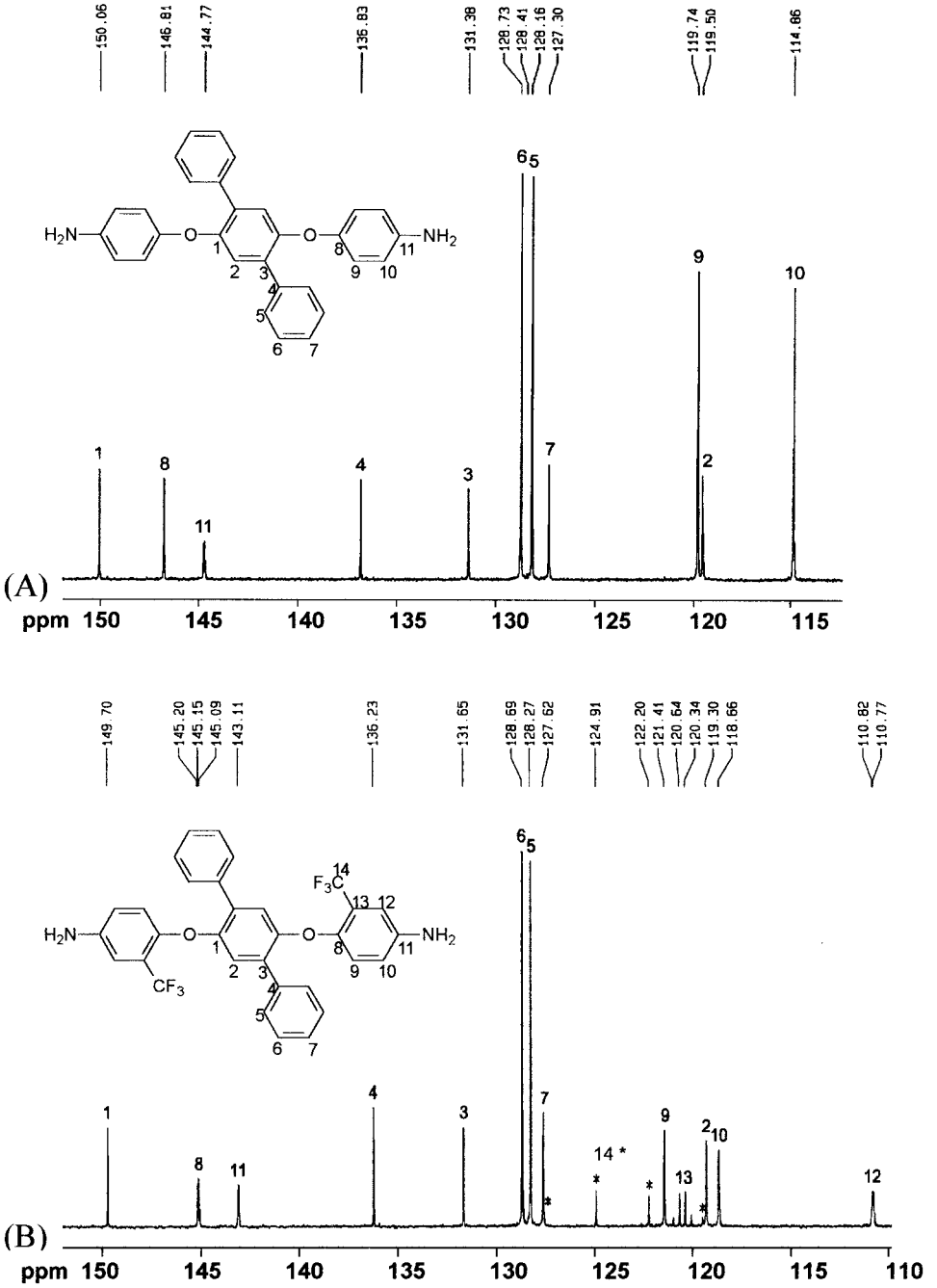

Figure 3. ^{13}C NMR (DMSO-d_6) spectra of (A) diamine **5a** and (B) diamine **5b**.

imides, only **9f** (from 6FDA) was soluble in THF and was characterized by GPC. For polyimide **9f**, M_n was 52,000, and M_w was 81,000.

The formation of polyimides was confirmed with IR spectroscopy and elemental analysis. All the polyimides exhibited characteristic imide group absorptions around 1780 (asymmetrical C═O stretch) and 1720 cm^{-1} (symmetrical C═O stretch), 1385 cm^{-1} (C—N stretch), and 1100 and 720 cm^{-1} (imide ring deformation), together with some strong absorption bands in the region of 1100–1300 cm^{-1} due to C—O and C—F stretching. The disappearance of amide and carboxyl bands at 1650–1700 and 2800–3500 cm^{-1} indicates a virtually complete conversion of the poly(amic acid) precursor into polyimide. The results

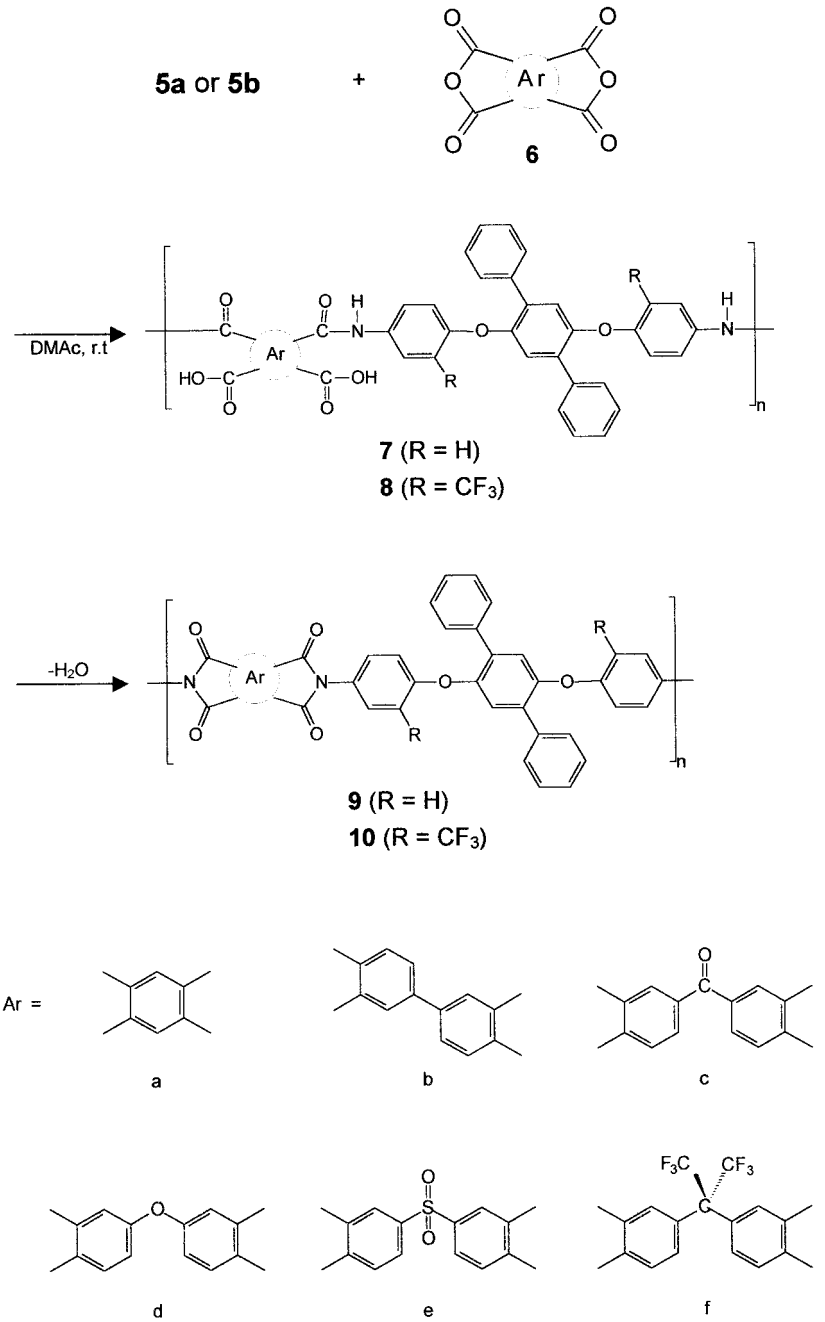

Scheme 2. Synthesis of polyimides from **5a** and **5b**.

of the elemental analyses of all the thermally cured polyimides are listed in Table 2. The values are generally in good agreement with the calculated values of the proposed structures.

Polymer Properties

Organosolubility

The organosolubility of the polyimides was determined qualitatively, and the results are listed in Table 3. The organosolubility behavior of the polyimides depended on their chain packing density and intermolecular interactions. Thus, the polyimides derived from more flexible dianhydrides such as ODPA, DSDA, and 6FDA generally displayed a higher solubility than those obtained from more rigid components such as PMDA, BPDA, and BTDA. As also shown in Table 3, the fluorinated polyimides **10a–10f** had relatively en-

Table 1. Inherent Viscosity (η_{inh}) of Poly(amic acid)s and Polyimides and Average Molecular Weights of THF-Soluble Polyimides[a]

Poly(amic acid)		Polyimide		GPC Data of Polyimides[c]		
Code	η_{inh} (dL/g)[b]	Code	η_{inh} (dL/g)[b]	M_n	M_w	M_w/M_n
7a	3.01	**9a**	–[d]	–[e]	–	–
7b	2.34	**9b**	–	–	–	–
7c	1.76	**9c**	–	–	–	–
7d	1.61	**9d**	–	–	–	–
7e	1.73	**9e**	0.67	–	–	–
7f	1.27	**9f**	0.55	52,000	81,000	1.54
8a	1.07	**10a**	–	–	–	–
8b	1.26	**10b**	1.33	42,000	67,000	1.62
8c	0.84	**10c**	0.63	45,000	71,000	1.59
8d	0.84	**10d**	0.62	69,000	97,000	1.41
8e	0.95	**10e**	0.62	79,000	100,000	1.28
8f	1.05	**10f**	0.83	45,000	71,000	1.58

[a] The polyimide samples were prepared via chemical imidization.
[b] Measured in DMAc at a concentration of 0.5 g/dL at 30 °C.
[c] With respect to polystyrene standards, with THF as the eluent.
[d] Insoluble in DMAc.
[e] Insoluble in THF.

hanced solubility compared to that of the corresponding polyimides **9a**–**9f** because of the introduction of the bulky CF_3 group, which further hindered dense chain packing and reduced chain–chain interactions. For the **9a**–**9f** series, only **9f**, derived from 6FDA, displayed good solubility. Polyimides **9a**–**9e** revealed a relatively lower solubility. However, the incorporation of 6FDA as a comonomer could impart solubility to the copolyimides, as reported in the literature.[27] Table 3 also shows the solubility of the polyimides prepared via chemical imidization by treatment with acetic anhydride and pyridine. The chemical imidization method may yield polyimides with a less dense packing structure, leading to an improvement in the solubility. The chemically imidized polyimides of the **10** series, except for **10a**, were readily soluble at room temperature in strongly polar solvents such as NMP, DMAc, and DMF and also in less polar solvents. In some cases, such as **10b** and **10c**, the polyimide samples prepared by chemical cyclodehydration exhibited better solubility than the thermally cured ones, and conformed with literature data.[36,37] The poor solubility of the thermally cured polyimides might be attributed to partial crosslinking within polymer chains or denser chain packing and aggregation during imidization at elevated temperatures.

Tensile Properties

All the polyimides except **9a** could produce good-quality and flexible films, and their tensile properties are summarized in Table 4. The polymer films had tensile strengths of 103–135 MPa, elongations to break of 8–14%, and tensile moduli of 1.85–2.35 GPa. All the polymers behaved as ductile materials with good tensile strengths and moderate elongations to break. Generally, the casting films of the **10a**–**10f** series exhibited slightly lower strengths and moduli than those of the **9a**–**9f** series, possibly because of increased free volume and reduced cohesive force caused by the CF_3 group.

X-Ray Diffraction Data

The crystallinity of the prepared polyimides was determined by WAXD measurements with graphite-monochromatized Cu Kα radiation. Both series of polymers showed almost completely amorphous diffraction patterns. This was reasonable because the polyimides contained laterally attached, noncoplanar *p*-terphenyl units that sterically disrupted the chain packing and inhibited significant chain–chain interactions. The amorphous nature of the **10** series polyimides could be attributed in part to the presence of the bulky CF_3 groups, which resulted in a less dense chain pack-

Table 2. Elemental Analysis of the Polyimides Prepared via Thermal Imidization

Polyimide	Formula (Formula Weight)		Elemental Analysis (%) of Polyimides C	H	N
9a	$(C_{40}H_{22}N_2O_6)_n$	Calcd.	76.17	3.54	4.47
	$(626.62)_n$	Found	75.39	3.53	3.99
9b	$(C_{46}H_{26}N_2O_6)_n$	Calcd.	78.12	3.73	3.99
	$(702.72)_n$	Found	77.64	3.71	3.60
9c	$(C_{47}H_{26}N_2O_7)_n$	Calcd.	76.75	3.59	3.83
	$(730.73)_n$	Found	76.22	3.57	3.44
9d	$(C_{46}H_{26}N_2O_7)_n$	Calcd.	76.37	3.65	3.90
	$(718.72)_n$	Found	75.77	3.58	3.59
9e	$(C_{46}H_{26}N_2O_8S)_n$	Calcd.	71.56	3.42	3.65
	$(766.78)_n$	Found	70.95	3.38	3.28
9f	$(C_{49}H_{32}N_2O_6F_6)_n$	Calcd.	68.53	3.73	3.26
	$(858.80)_n$	Found	68.24	3.59	3.18
10a	$(C_{42}H_{20}N_2O_6F_6)_n$	Calcd.	66.15	2.64	3.67
	$(762.62)_n$	Found	65.59	2.60	3.26
10b	$(C_{48}H_{24}N_2O_6F_6)_n$	Calcd.	68.74	2.88	3.34
	$(838.71)_n$	Found	68.11	2.83	2.96
10c	$(C_{49}H_{24}N_2O_7F_6)_n$	Calcd.	67.90	2.79	3.23
	$(866.72)_n$	Found	67.25	2.74	2.84
10d	$(C_{48}H_{24}N_2O_7F_6)_n$	Calcd.	67.45	2.83	3.28
	$(854.71)_n$	Found	66.97	2.81	3.01
10e	$(C_{48}H_{24}N_2O_8SF_6)_n$	Calcd.	63.86	2.68	3.10
	$(902.77)_n$	Found	63.28	2.65	2.83
10f	$(C_{51}H_{33}N_2O_6F_{12})_n$	Calcd.	61.51	3.02	2.81
	$(994.83)_n$	Found	61.59	2.94	2.67

ing structure. Figure 4 compares the WAXD patterns of some structurally related polyimides. As reported in a previous publication,[38] the polyimides PMDA/TPEQ and BPDA/TPEQ derived from 1,4-bis(4-aminophenoxy)benzene [triphenyl ether hydroquinone diamine (TPEQ)] showed semicrys-

Table 3. Solubility Behavior of Thermally Imidized/Chemically Imidized Polyimides

Polyimide	Solvent[a] NMP	DMAc	DMF	DMSO	*m*-Cresol	THF	$CHCl_3$
9a	−/−	−/−	−/−	−/−	−/−	−/−	−/−
9b	−/−	−/−	−/−	−/−	−/+h	−/−	−/−
9c	−/−	−/−	−/−	−/−	−/−	−/−	−/−
9d	+h/+h	−/−	−/−	−/−	+h/+	−/−	+/+
9e	+h/+h	+/+h	−/−	−/−	+h/+h	−/−	+h/+h
9f	+/+	+/+	+/+	+/+	+/+	+/+	+/+
10a	−/−	−/−	−/−	−/−	−/−	−/−	−/−
10b	−/+	+h/+	−/−	−/+	+h/+h	+h/+	−/−
10c	−/+	+h/+	+h/+	−/+h	−/+h	−/+	−/−
10d	+h/+	+/+	+/+	−/−	+h/+h	+/+	+/+
10e	+/+	+/+	+/+	−/+	+h/+h	+/+	+h/+h
10f	+/+	+/+	+/+	+h/+	+h/+h	+/+	+/+

[a] The qualitative solubility was tested with 10 mg of a sample in 1 mL of a solvent. + = soluble at room temperature; +h = soluble on heating at 100 °C; − = insoluble even on heating.

Table 4. Thin-Film Tensile Properties of the Polyimides

Polymer	Tensile Strength (MPa)	Elongation to Break (%)	Tensile Modulus (GPa)
9a	—[a]	—	—
9b	122	8	2.31
9c	130	10	2.35
9d	126	13	2.17
9e	116	9	1.99
9f	117	9	2.07
10a	112	12	1.89
10b	135	14	2.05
10c	111	8	2.17
10d	117	10	2.01
10e	103	8	2.11
10f	108	10	1.93

[a] The film was too brittle to be tested.

talline patterns. In contrast, the corresponding pendent-group-containing polyimides **8a**, **8b**, **10a**, and **10b** displayed amorphous patterns. From this comparison, an obvious effect of the introduction of the pendent phenyl groups or both phenyl and CF_3 groups on the crystallinity of these polyimides can be confirmed.

Optical Transparency

Thin films were measured for optical transparency with UV–vis spectroscopy. The UV–vis spectra of all the polyimide films from the UV–vis spectra are shown in Figure 5. All the fluorinated polyimides showed a lower cutoff wavelength [absorption edge (λ_0)] and higher optical transparency than their respective CF_3-free analogues. The polyimide films of **10d** and **10f**, produced from ODPA and 6FDA, respectively, were nearly colorless, and this may be explained by the reduction of the intermolecular charge-transfer complex (CTC) between alternating electron-donor (diamine) and electron-acceptor (dianhydride) moieties. The low adsorbance of the polyimides with the CF_3 groups in their diamine moieties can also be explained by the reduced intermolecular

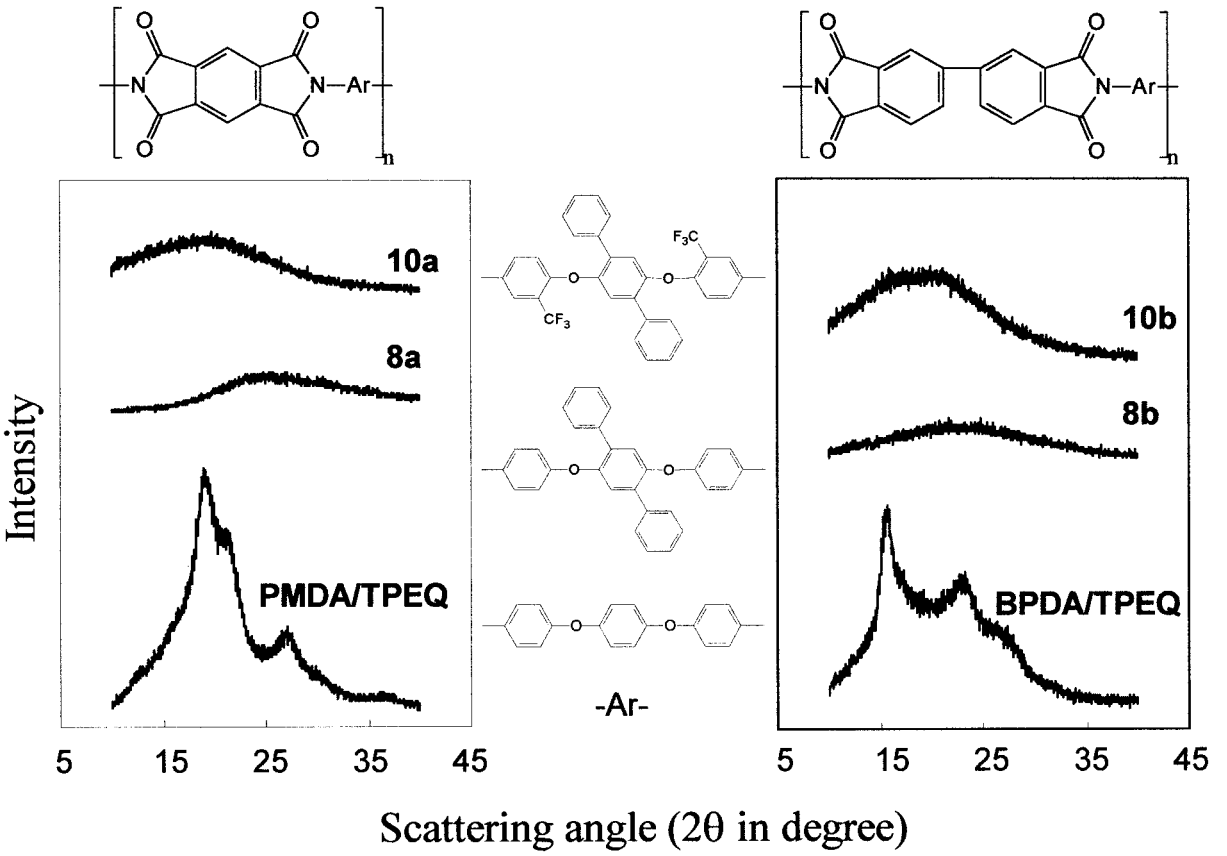

Figure 4. Effect of the pendent groups on the crystallinity of PMDA and BPDA polyimides.

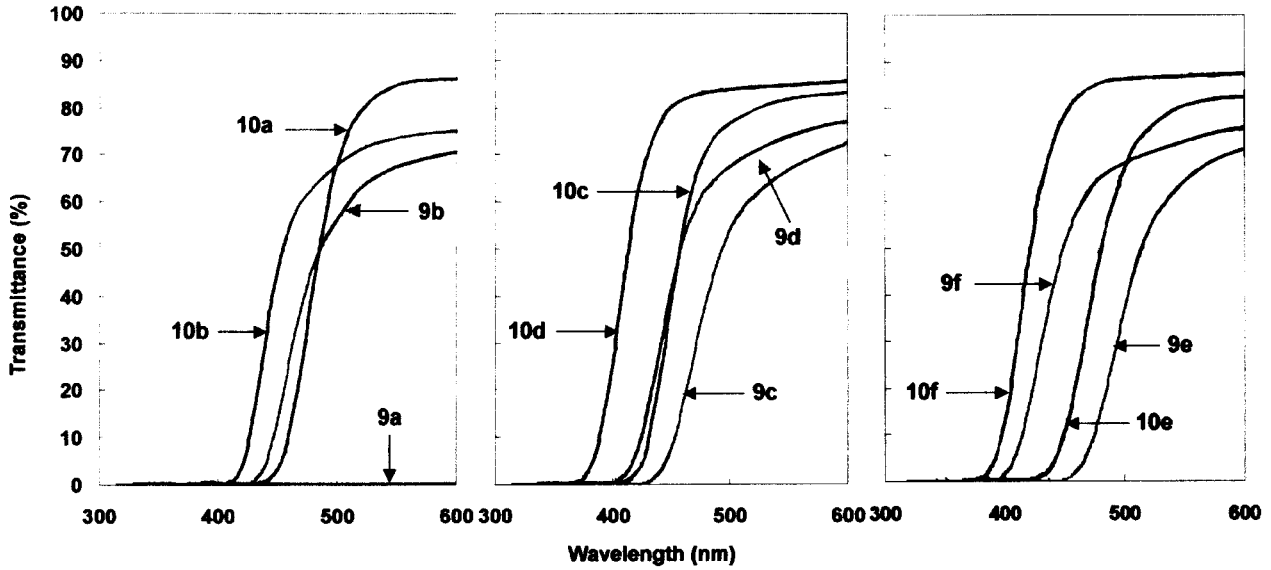

Polymer code	9a	9b	9c	9d	9e	9f	10a	10b	10c	10d	10e	10f
λ_0	—	421	433	405	445	394	436	402	411	373	423	370

Figure 5. UV–vis spectra of polyimide films (film thickness = 50–80 μm).

interactions. The bulky and electron-withdrawing CF_3 group in diamine moieties was effective in reducing CTC formation between polymer chains through steric hindrance and the inductive effect (by decreasing the electron-donating property of diamine moieties). A secondary positive effect of the CF_3 groups on the film transparency was the weakened intermolecular cohesive force due to the lower polarizability of the C—F bond. The decrease in intermolecular CTC formation is understandable also from the significant solubility of the **10** series polyimides with the CF_3 substituents.

Thermal Properties

DSC, TMA, and TGA were used to investigate the thermal properties of the polyimides films, and some of the thermal behavior data are reported in Table 5. In the DSC experiments, all the polymers were rapidly cooled from 400 to 50 °C to form predominantly amorphous samples, and distinct glass transitions could be observed in the subsequent heating DSC traces. The T_g values of polyimides **9a–9f** and **10a–10f** were recorded in the ranges of 250–302 and 254–308 °C, respectively. In general, T_g's are affected by both molecular packing and chain rigidity. As expected, in each series, the polyimide obtained from ODPA showed the lowest T_g because of the presence of a flexible ether linkage between the phthalimide units, and the polyimide derived from PMDA had the highest T_g because of the rigid pyromellitimide unit. The T_s (or apparent T_g) values of the polyimide films were measured by the TMA method with a loaded penetration probe. They were obtained from the onset temperatures of the probe displacement on the TMA traces. In most cases, the T_s values determined by TMA were comparable to the T_g values determined by the DSC technique. When the two series of polyimides were compared, the **10a–10f** series polyimides generally revealed slightly higher T_g and T_s values than their **9** series counterparts. This might be a result of higher steric hindrance of segmental mobility caused by the CF_3 groups, although they might result in higher free volume and weaken the interchain interactions, which should reduce T_g. In addition, polyimides **10a–10f** showed higher T_g values (12–26 °C) than those of structurally similar fluorinated polyimides obtained from 1,4-bis(4-amino-2-trifluoromethylphenoxy)benzene by Yang's group.[30] This could be explained in terms of an increased rotational barrier due to the laterally attached *p*-terphenyls.

Table 5. Thermal Properties of the Polyimides

Polyimide	T_g (°C)[a]	T_s (°C)[b]	$T_{5\%\ wt\ loss}$ (°C)[a]		$T_{10\%\ wt\ loss}$ (°C)[c]		Char Yield (%)[d]
			In N_2	In Air	In N_2	In Air	
9a	302	291	560	519	583	550	57
9b	271	270	579	536	597	588	63
9c	256	252	557	534	581	579	64
9d	250	251	552	525	574	568	60
9e	270	273	519	543	549	576	57
9f	263	260	549	540	571	567	64
10a	308	299	587	573	610	598	61
10b	276	276	591	566	615	594	63
10c	263	259	573	554	601	589	61
10d	254	253	589	560	615	590	60
10e	273	272	510	527	546	558	57
10f	267	270	554	546	576	567	53

[a] Midpoint temperature of the baseline shift on the second DSC heating trace of a sample after quenching from 400 °C.
[b] Softening temperature taken as the onset temperature of the probe displacement on the TMA trace at a heating rate of 10 °C/min. The film samples were heated at 300 °C for 1 h before the TMA experiments.
[c] Recorded by TGA at a heating rate of 20 °C/min.
[d] Residual weight percentage at 800 °C in nitrogen.

The thermal and thermooxidative stabilities of these polyimides were evaluated by TGA under both nitrogen and air atmospheres with a 5 or 10 wt % loss temperature for comparison. Typical TGA thermograms for polyimides **9a** and **10a** are shown in Figure 6. The decomposition temperatures (T_d's) at a 10% weight loss of polyimides **10a–10f** were recorded in the range of 546–615

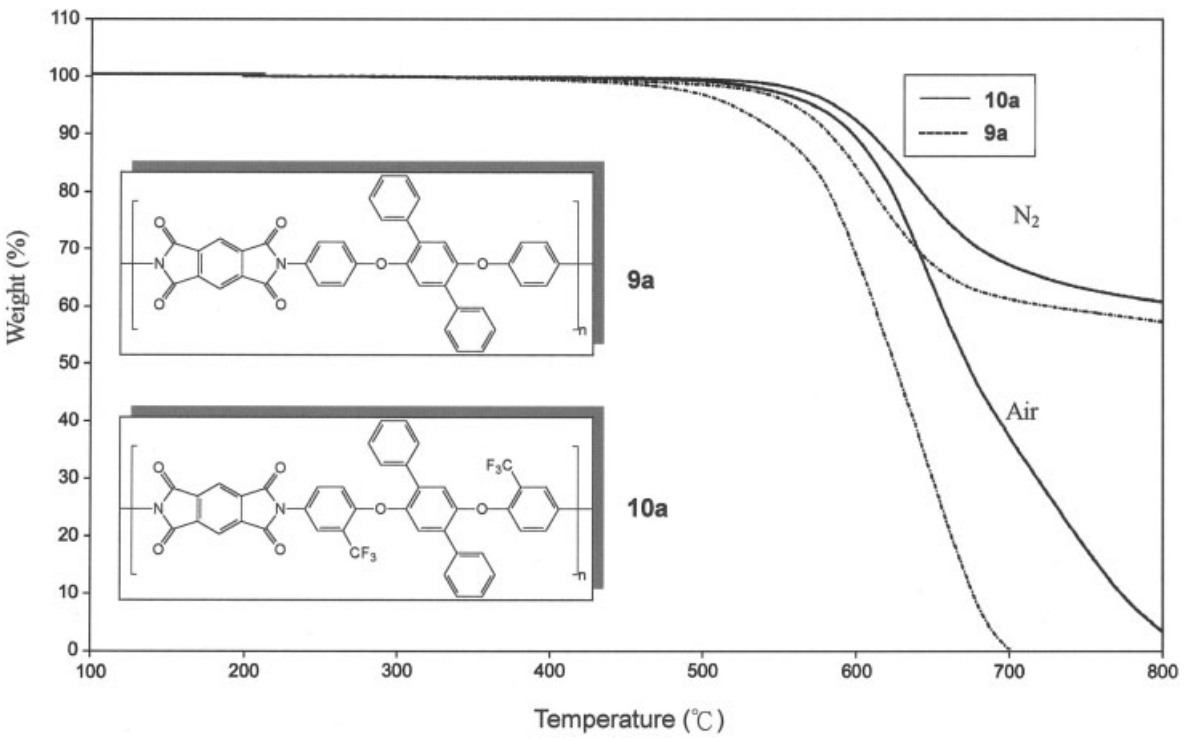

Figure 6. TGA curves of polyimides **9a** and **10a** at a heating rate of 20 °C/min.

Table 6. Moisture Absorption and Dielectric Constants of the Polyimides

Polyimide	Film Thickness (μm)	Moisture Absorption (%)	Dielectric Constant (Dry)		
			1 kHz	10 kHz	1 MHz
9a	78	2.4	3.45	3.31	3.28
9b	78	1.8	3.66	3.52	3.48
9c	76	1.7	3.42	3.42	3.37
9d	79	1.9	3.19	3.17	3.13
9e	66	2.6	3.34	3.29	3.25
9f	80	0.5	3.17	2.99	2.96
10a	78	2.2	3.12	3.06	2.98
10b	67	1.4	3.42	3.40	3.34
10c	53	1.3	3.17	3.16	3.10
10d	53	1.3	3.22	3.21	3.14
10e	71	2.2	3.24	3.21	3.16
10f	63	0.4	2.89	2.87	2.83
Ref[a]	80	2.1	3.89	3.85	3.67

[a] A reference polyimide prepared from PMDA and 4,4′-oxydianiline [η_{inh} of the poly(amic acid) precursor = 2.90 dL/g].

°C in nitrogen and in the range of 558–598 °C in air, and those of polyimides **9a**–**9f** were recorded in the range of 549–597 °C in nitrogen and in the range of 550–588 °C in air. Most of the fluorinated polyimides **10a**–**10f** exhibited higher T_d values than their analogous **9a**–**9f** counterparts, and this increase may be a result of stronger C—F bonding of the CF_3 groups. All the polyimides left more than 53% char yields at 800 °C in nitrogen. The TGA results showed an excellent thermal stability of these polyimides, even though they revealed high solubility.

Moisture Absorption and Dielectric Constants

The moisture absorption and dielectric constants of all the polyimides are reported in Table 6. In comparison, the fluorinated polyimides **10a**–**10f** exhibited lower moisture absorption and dielectric constants than the corresponding **9a**–**9f** analogues and the standard PMDA/4,4′-oxydianiline polyimide film. The moisture absorption and dielectric constant were minimized for polyimide **10f**, in which both the dianhydride and diamine moieties in the polymer chain contained the hydrophobic fluorine groups. The reduced dielectric constants might be attributable to the presence of bulky CF_3 substituents and the lateral *p*-terphenyl units, which resulted in less efficient chain packing and increased free volume. In addition, the strong electronegativity of fluorine resulted in permanent dipole moments of the C—F bonds, thereby reducing the dielectric constant.

CONCLUSIONS

A novel fluorinated diamine (**5b**) was synthesized via a high-yielding two-step procedure. A series of novel fluorinated polyimides with high molecular weights were obtained successfully from **5b** with various aromatic dianhydrides by two-step thermal or chemical imidization methods. The obtained polyimides displayed high solubility, excellent thermal stability, good film-forming processability and mechanical properties, and low dielectric constants. The good combination of properties and processability exhibited in this series of polyimides demonstrates their potential for future high-performance materials.

The authors thank the National Science Council of the Republic of China for its financial support (NSC 92-2216-E-036-003).

REFERENCES AND NOTES

1. Polyimides; Wilson, D.; Stenzenberger, H. D.; Hergenrother, P. M., Eds.; Chapman & Hall: New York, 1990.
2. Polyimides: Fundamentals and Applications; Ghosh, M. K.; Mittal, K. L., Eds.; Marcel Dekker: New York, 1996.
3. Huang, S. J.; Hoyt, A. E. TRIP 1995, 3, 262.
4. de Abajo, J.; de la Campa, J. G. In Progress in Polyimide Chemistry I; Kricheldorf, H. R., Ed.; Springer: Berlin, 1999; pp 23–59.

5. Hsiao, S.-H.; Yang, C.-P.; Fan, J.-C. J Polym Res 1994, 1, 345.
6. Tamai, S.; Yamaguchi, A.; Ohta, M. Polymer 1996, 37, 3683.
7. Hsiao, S.-H.; Huang, P.-C. J Polym Res 1997, 4, 189.
8. Imai, Y. High Perform Polym 1995, 7, 337.
9. Hsiao, S.-H.; Li, C.-T. Macromolecules 1998, 31, 7213.
10. Liaw, D.-J.; Liaw, B.-Y.; Lai, S.-H. Macromol Chem Phys 2001, 202, 807.
11. High-Performance Polymers 2: Polyquinoxalines and Polyimides; Rabilloud, G., Ed.; Editions Technip: Paris, 1999; pp 199–250.
12. Li, F.; Ge, J. J.; Honigfort, P. S.; Fang, S.; Chen, J.-C.; Harris, F. W.; Cheng, S. Z. D. Polymer 1999, 40, 4987.
13. Eastmond, G. C.; Paprotny, J. Macromolecules 1995, 28, 2140.
14. Hsiao, S.-H.; Yang, C.-P.; Chu, K.-Y. Macromolecules 1997, 30, 165.
15. Hsiao, S.-H.; Yang, C.-P.; Chen, S.-H. J Polym Sci Part A: Polym Chem 2000, 38, 1551.
16. Hsiao, S.-H.; Yang, C.-Y. Macromol Chem Phys 1997, 198, 2181.
17. Hsiao, S.-H.; Yang, C.-P.; Yang, C.-Y. J Polym Sci Part A: Polym Chem 1997, 35, 1487.
18. Reddy, D. S.; Hsu, C.-F.; Wu, F.-I. J Polym Sci Part A: Polym Chem 2002, 40, 262.
19. Chou, C.-H.; Reddy, D. S.; Hsu, C.-F. J Polym Sci Part A: Polym Chem 2002, 40, 3615.
20. Reddy, D. S.; Chou, C.-H.; Hsu, C.-F.; Lee, G.-H. Polymer 2003, 44, 557.
21. Spiliopoulos, I. K.; Mikroyannidis, J. A. Macromolecules 1996, 29, 5313.
22. Spiliopoulos, I. K.; Mikroyannidis, J. A.; Tsivgoulis, G. M. Macromolecules 1998, 31, 522.
23. Mikroyannidis, J. A. J Polym Sci Part A: Polym Chem 1999, 37, 15.
24. Mikroyannidis, J. A. Polymer 1999, 40, 3107.
25. Spiliopoulos, I. K.; Mikroyannidis, J. A. J Polym Sci Part A: Polym Chem 2002, 40, 2591.
26. Sato, M.; Nakashima, S.; Uemoto, Y. J Polym Sci Part A: Polym Chem 2003, 41, 2676.
27. Xu, J.-W.; He, C.-B.; Chung, T.-S. J Polym Sci Part A: Polym Chem 2001, 39, 2998.
28. Sasaki, S.; Nishi, S. In Polyimides: Fundamentals and Applications; Ghosh, M. K.; Mittal, K. L., Eds.; Marcel Dekker: New York, 1996; pp 71–120; see also references therein.
29. Hougham, G. In Fluoropolymers 2: Properties; Hougham, G.; Cassidy, P. E.; Johns, K.; Davidson, T., Eds.; Kluwer Academic/Plenum: New York, 1999; pp 233–276.
30. Xie, K.; Zhang, S. Y.; Liu, J. G.; He, M. H.; Yang, S. Y. J Polym Sci Part A: Polym Chem 2001, 39, 2581.
31. Yang, C.-P.; Hsiao, S.-H.; Hsu, M.-F. J Polym Sci Part A: Polym Chem 2002, 40, 524.
32. Banerjee, S.; Madhra, M. K.; Salunke, A. K.; Maier, G. J Polym Sci Part A: Polym Chem 2002, 40, 1016.
33. Hsiao, S.-H.; Yang, C.-P.; Chung, C.-L. J Polym Sci Part A: Polym Chem 2003, 41, 2001.
34. Hougham, G.; Tesoro, G.; Viehbeck, A. Macromolecules 1996, 29, 3453.
35. Zhao, L.; He, C.-B.; Lu, Z.-H.; Chung, T.-S. J Polym Sci Part A: Polym Chem 2001, 39, 1288.
36. Xie, K.; Liu, J. G.; Zhou, H. W.; Zhang, S. Y.; He, M. H.; Yang, S. Y. Polymer 2001, 42, 7267.
37. Zhou, H. W.; Liu, J. G.; Qian, Z. G.; Zhang, S. Y.; He, M. H.; Yang, S. Y. J Polym Sci Part A: Polym Chem 2001, 39, 2404.
38. Hsiao, S.-H.; Chen, Y.-J. Eur Polym J 2002, 38, 815.